Facultad de **Medicina**

GRADO EN CIENCIAS BIOMÉDICAS

TRABAJO FIN DE GRADO

Escribir Título TFG en Castellano

Papel de BAMBI, un regulador de la señalización de TGF-beta, en homeostasis e inflamación

Escribir Título TFG en Inglés

The role of BAMBI in TGF-beta signaling during homeostasis and inflammation

Autor/a: Paula Bermúdez Revuelta

Director/a: Ramón Merino Pérez

Co-director/a: Luis Gil de Gómez Sesma

Co-director/a:

Santander, 7 June 2025

Index

Trabajo de Fin de Grado
Grado en Ciencias Biomédicas · Facultad de Medicina
2024 – 2025

The role of BAMBI in TGF-β signaling during homeostasis and inflammation

GRAPHICAL ABSTRACT

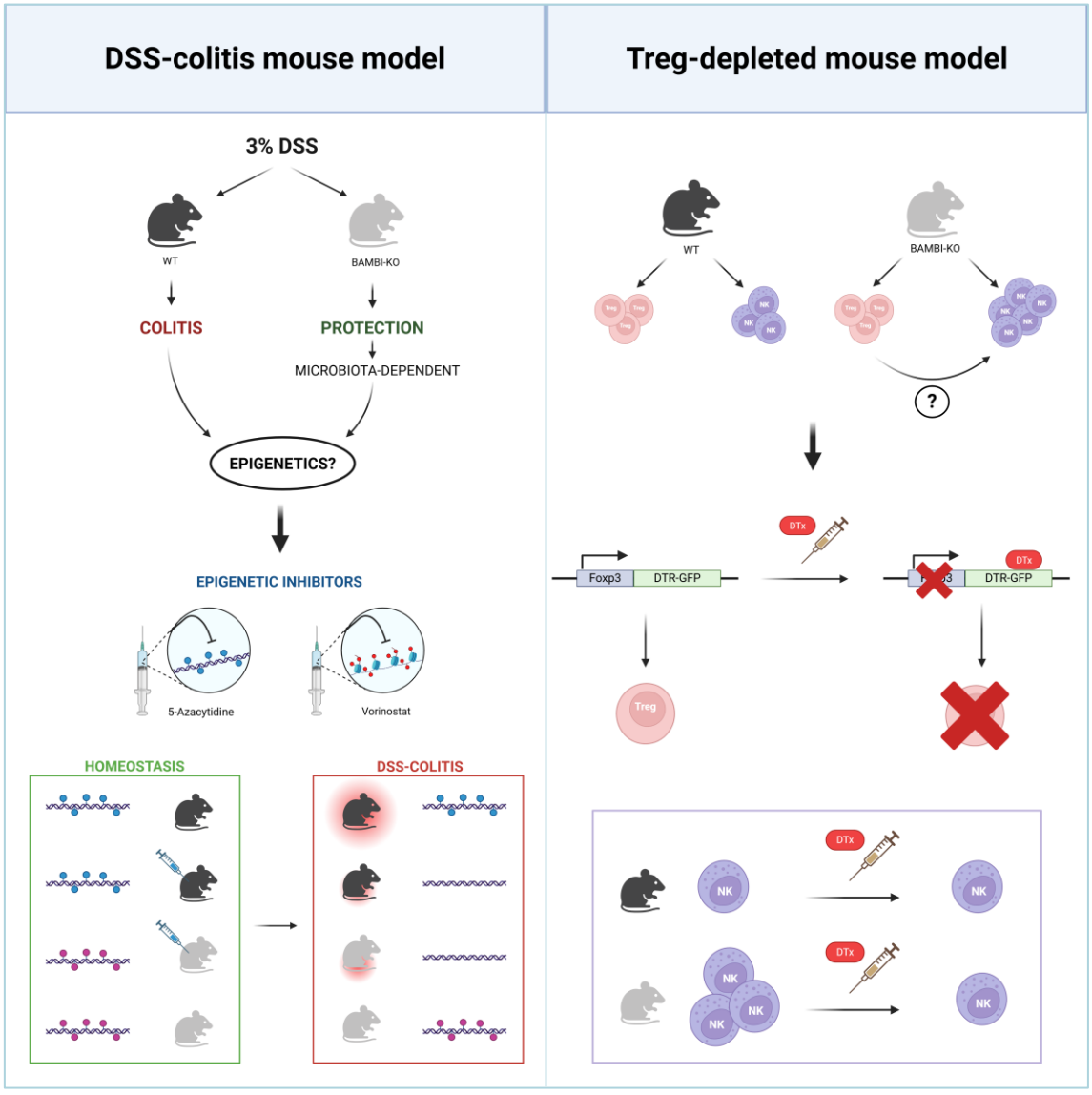

AUTHORS

Paula Bermúdez Revuelta, Ramón Merino Pérez, Luis Gil de Gómez Sesma

Correspondence: paula.bermudez@alumnos.unican.es

UC | Universidad de Cantabria

Trabajo de Fin de Grado
Grado en Ciencias Biomédicas · Facultad de Medicina
2024 – 2025

The role of BAMBI in TGF-β signaling during homeostasis and inflammation

Paula Bermúdez Revuelta[1], Ramón Merino Pérez[2], Luis Gil de Gómez Sesma[1]

[1]Facultad de Medicina, Universidad de Cantabria, Santander
[2]Instituto de Biomedicina y Biotecnología de Cantabria (IBBTEC) - CSIC

* Correspondence: ramon.merino@unican.es; luis.gildegomez@unican.es

RESUMEN

BMP and Activin Membrane-Bound Inhibitor (BAMBI) es una proteína transmembrana que regula negativamente la señalización de TGF-β, modulando la diferenciación de células T $CD4^+$ hacia células T reguladoras (Tregs) o Th17. En ratones BAMBI-KO este equilibrio se desplaza hacia las Tregs, contribuyendo a la protección contra enfermedades autoinmunes en modelos de ratón.

Estudios anteriores han descrito que la ausencia de BAMBI también confiere protección contra la colitis ulcerosa. Puesto que la microbiota es imprescindible en este efecto, investigamos si las modificaciones epigenéticas también participan en la respuesta protectora. Nuestros resultados muestran que los inhibidores epigenéticos anulan el fenotipo protector observado en ratones BAMBI-KO. Esto sugiere que, en ausencia de BAMBI, modificaciones epigenéticas, probablemente influenciadas por el microbioma intestinal, definen un programa necesario para prevenir el desarrollo de colitis.

A diferencia de otras patologías, la protección contra colitis en los ratones BAMBI-KO no está mediada por Tregs. Para entender la relevancia de esta población, eliminamos las Tregs y observamos que en ausencia de BAMBI hay una distribución diferente de células T efectoras y NKs.

En conjunto, estos resultados nos acercan a dilucidar el mecanismo implicado en el efecto protector de la inhibición de BAMBI y su potencial terapéutico en enfermedades autoinmunes.

ABSTRACT

BMP and Activin Membrane-Bound Inhibitor (BAMBI) is a transmembrane protein that negatively regulates TGF-β signaling and, thereby modulates the differentiation of $CD4^+$ T cells to either regulatory T-cells (Tregs) or Th17 cells. In BAMBI-KO mice this balance is shifted towards Tregs, contributing to protection against autoimmune diseases in mouse models.

Previous studies have shown that BAMBI deficiency also confers protection against ulcerative colitis. Since microbiota, that rules the gut microenvironment by different mechanisms, is pivotal in this effect, we investigated whether epigenetic modifications are involved in the better outcome of BAMBI-deficient mice. Our results show that epigenetic inhibitors abrogate the protective phenotype observed in BAMBI-KO mice. These findings suggest that, in the absence of BAMBI, epigenetic modifications, probably through the influence of gut microbiome, define a transcriptional program essential for preventing the development of colitis.

Unlike other pathologies, protection against colitis in BAMBI-KO mice is not Treg-dependent. To understand the relevance of this population, we depleted Tregs, and we observed differential distribution of effector T-cells and NK cells in the absence of BAMBI.

Together, these results add relevant information to elucidate the mechanism involved in the protective effect of BAMBI inhibition and its therapeutical potential for inflammatory and autoimmune diseases.

KEYWORDS

BAMBI, TGF-β, ulcerative colitis, microbiota, epigenetic modifications, immune response, Treg cells, tolerance, NK cells

INTRODUCTION

The immune system (IS) consists of a complex network of cells and proteins working together to protect the host from infections, diseases and foreign substances (antigens). There are two branches of the IS that cooperate in the immune response, the innate immune system and the adaptive immune system. Innate immunity is a rapid response that constitutes the first line of defense. It is composed of different immune cells such as Natural Killer (NK) cells and antigen-presenting cells (APCs) like macrophages and dendritic cells.[1] While APCs present captured antigens from the environment, NK cells are cytotoxic lymphocytes that play an essential role in viral infections and tumors. Upon activation, innate immunity stimulates the adaptive immune system by secreting soluble proteins called cytokines.[2]

The adaptive immune system develops a specific immune response and retains immunological memory. It is divided into two types, humoral and cell mediated adaptive immune systems. B and T lymphocytes are the main cells of each group respectively.[1] B lymphocytes are essential components of the adaptive immune system, particularly of humoral immunity. Its main function is the production of antibodies, but these cells also have other functions such as cytokine production. B cells contribute to the activation of T cells, by acting as APCs, and they can also differentiate into memory B cells.[3]

T lymphocytes are the main effector cells in cellular immunity. T cells are divided into two major groups, $CD8^+$ and $CD4^+$ T cells. $CD8^+$ T lymphocytes have cytotoxic activity and act against virus-infected, bacteria-infected or cancer cells.[4] On the other hand, $CD4^+$ T lymphocytes regulate different immune cells by producing cytokines. $CD4^+$ T cells are also called helper T (Th) cells, and there are many subtypes with different functions.[5] Moreover, there has been identified another lymphocyte population, memory T (Tm) cells. These cells are antigen-experienced T lymphocytes which provide rapid immune response against re-exposure to the same pathogen. Tm cells are classified into two main groups, central memory T (Tcm) cells and effector memory T (Tem) cells. Tcm cells reside in secondary lymphoid organs such as the spleen, whereas Tem cells are found in peripheral tissues and in the blood.[6]

Regarding T lymphocytes, the balance between two $CD4^+$ T cell subpopulations, T helper 17 (Th17) and regulatory T (Treg) cells, is essential for maintaining homeostasis. Th17 cells are proinflammatory cells which combat extracellular bacteria and fungi. Autoimmune diseases are often originated by the hyperactivation of Th17 cells.[7] In contrast, Treg cells are suppressive cells key in tolerance that control the activity of other immune cells like Th17 cells. Forkhead box P3 (Foxp3) is a transcription factor involved in the differentiation of Treg cells. It is indispensable for the development, metabolism and function of these cells, and its deficiency could induce an autoimmune lymphoproliferative syndrome.[8]

The differentiation of both Th17 cells and Treg cells is regulated by the transforming growth factor beta (TGF-β) depending on the surrounding cytokine environment.[7] TGF-β is a pleiotropic cytokine that belongs to the TGF-β superfamily, a large group composed of five subfamilies of structurally related proteins including activins, inhibins, Bone Morphogenetic Proteins (BMPs), Growth Differentiation Factors (GDFs), Müllerian Inhibiting Substance (MIS) and TGF-βs. Members of this superfamily are involved in regulating immune responses, maintaining tissue homeostasis and controlling cellular proliferation, differentiation, and apoptosis.[9] TGF-β is a bifunctional regulator capable of either stimulating or inhibiting cell proliferation. Thus, in an environment of pro-inflammatory cytokines such as IL-23, IL-1β, or IL-21, TGF-β promotes Th17 cell

differentiation contributing to the development of autoimmune diseases. In contrast, in the absence of these signals and in the presence of IL-2, TGF-β maintains immune homeostasis by inducing the differentiation of Treg cells with anti-inflammatory functions.[10,11]

Bone Morphogenetic Protein and Activin Membrane-Bound Inhibitor (BAMBI) is a 260-amino acid transmembrane glycoprotein that shares structural homology with TGF-β type I receptors. However, BAMBI has a different intracellular domain, it is shorter and lacks a serine/threonine kinase domain. As a result, it cannot initiate phosphorylation-dependent signaling. BAMBI forms non-functional heterodimers with TGF-β type I receptors, acting as a pseudoreceptor that interferes with both TGF-β and BMP signaling pathways.[12] It has been reported that, in the absence of BAMBI in BAMBI Knockout (BAMBI-KO) mice, the Th17/Tregs ratio is shifted towards Tregs differentiation. Therefore, BAMBI has been associated with autoimmune diseases, and it has been demonstrated that BAMBI inhibition prevents the progression of autoimmune diseases such as Psoriatic Arthritis (PsA) through mechanisms that are dependent on Treg cells and TGF-β signaling.[13]

Additionally, BAMBI also influences the function and differentiation of various immune cell populations such as other T lymphocytes subpopulations, B lymphocytes and NK cells.[14] Although BAMBI-KO mice showed protection against inflammatory processes, the absence of BAMBI in homeostasis stimulated T cell proliferation and NK activity emphasizing the dual role of TGF-β and the relevance of tolerance mechanisms in the protection against autoimmune and inflammatory diseases.[13]

Ulcerative colitis (UC) is one of the two types of inflammatory bowel disease (IBD). It is a chronic, idiopathic condition characterized by relapsing and remitting episodes that affect the colon. It is mainly identified by symptoms such as bloody diarrhea, abdominal pain, fecal incontinence and weight loss. Unlike Chron's disease (CD), which can affect any part of the gastrointestinal tract, UC is restricted to the large intestine leading to continuous inflammation of the colonic mucosa. Its inflammation typically starts in the distal colon and may extend proximally.[15]

The prevalence and incidence of UC have significantly increased over the last century, currently affecting 5 million people worldwide. Around 0.2% of the European population is affected, with Spain reporting an incidence of approximately 0.1%.[16] The etiology remains unknown, but it is believed to result from complex interactions between environmental factors, the immune system, gut microbiota, and genetic susceptibility. To this day, available treatments focus on reducing recurrent inflammation of the intestinal mucosa since there is no cure for the disease. Colonoscopy remains the most efficient diagnostic test, and common treatments options include 5-aminosalicylates, corticosteroids and immunosuppressants (thiopurines, methotrexate, and 6-mercaptopurine).

UC has become a global concern due to its rising incidence and the lack of reliable diagnostic tests and affordable, effective treatments. Thus, there is a need to identify novel therapeutic targets to enable the development of more efficient and accessible treatments. In this scenario, studying the interaction between the immune system and the gut microbiota has gained considerable importance.[17]

The gut microbiota consists of numerous species of bacteria, viruses and fungi, forming the largest symbiotic ecosystem with the host. The relationship between the IS and the microbiota is bidirectional and highly dynamic. Over thousands of years of co-evolution, they have established a state of commensalism that benefits both the microorganisms and the host, and it is essential for maintaining homeostasis.[18] In this context, the intestinal epithelium (IEp) acts as a passive physical barrier that separates the two compartments and participates in the crosstalk between microbiota and immune cells. Hence, the maintenance of intestinal homeostasis depends on the equilibrium between microbiota and the IS. When this equilibrium is disrupted, dysbiosis appears, leading to inflammation and abnormal immune responses.[19]

Intestinal homeostasis is maintained through a complex network of cellular and molecular interactions between the gut microbiota, the IS and the IEp. Immune cells, cell-cell interactions, receptors, cytokines, and other signals, work together to sustain this equilibrium.[19] In this regard, TGF-β plays a crucial role. TGF-β signaling is essential for preserving the integrity of the intestinal epithelial barrier and for modulating the interaction between the IS and the gut microbiota. Dysregulation of TGF-β signaling has been implicated in the pathogenesis of several inflammatory and autoimmune diseases, including IBDs.[20]

Based on the relevance of TGF-β, our laboratory group had initiated the characterization of the role of BAMBI in the regulation of intestinal homeostasis. Dextran Sulfate Sodium (DSS) is a toxic sulphated polysaccharide commonly used to induce IBD in animal models.[21] This model is especially relevant since although DSS was administered orally via drinking water, lesions were predominantly observed in the colon, a region with high BAMBI expression. Our previous results showed that wild type (WT) mice developed colitis whereas BAMBI-KO mice were protected from disease.

As the absence of BAMBI promotes the differentiation of Treg cells, and these cells prevent autoimmune diseases,[13] our group has done DSS-colitis experiments with Treg depletion. Interestingly, unlike other autoimmune and inflammatory models, Treg depletion did not revert the protection observed in BAMBI-KO mice. This data suggested that protection against DSS-colitis in BAMBI-KO mice was not mediated by the immune-suppressive function of Tregs cells. In addition, these results observed in a conventional animal facility were not replicated under Specific Pathogen Free (SPF) conditions, where both WT and BAMBI-KO mice developed colitis demonstrating that colon microbiota play a key role in this protective effect. In fact, preliminary data show different alterations in gene expression and epigenetic modifications in colonic intestinal epithelial cells (IECs) from WT mice compared to BAMBI-KO mice. Together, these findings suggest that BAMBI modulates via TFG-β the direct crosstalk between the IEp and the gut microbiota, and further investigations are required to evaluate the molecular and cellular mechanisms involved.

To investigate the underlying epigenetic mechanisms, WT and BAMBI-KO mice were treated with 5-azacytidine (5-AZA), a DNA methylation inhibitor which was the first agent approved by the Food and Drug Administration (FDA) for myelodysplastic syndromes;[22] suberoylanilide hydroxamic acid (SAHA, also known as Vorinostat (VOR)), a histone deacetylase (HDAC) inhibitor which was the first HDAC inhibitor approved by the FDA and is currently used in cancer therapy,[23] and the combination of both drugs.

With the present study, we aimed to understand the role of BAMBI in non-Treg dependent inflammatory diseases. Additionally, due to the relevance of Tregs in the

protection against autoimmune diseases, we further explored its function in maintaining homeostasis. In this context, since BAMBI-KO mice show an expansion of mature and activated peripheral lymphocytes including T cells and NK cells under physiological conditions, we aimed to determine whether the protective effect observed in BAMBI-KO mice would be maintained in the absence of Tregs, by comparing responses between WT and BAMBI-KO animals after Treg depletion.

RESULTS

Our preliminary data show that colitis development is prevented in the absence of BAMBI in a microbiome-dependent manner. Microbiota and its derivates are essential for intestinal homeostasis and this effect is mediated by gene expression and metabolic modifications. Since this protection is not mediated by Tregs, we hypothesize that alternative tolerogenic mechanisms based on a specific epigenetic program are involved in this effect. Conversely, depletion of Tregs abrogates the anti-inflammatory profile of BAMBI-KO mice in other pathologies. However, it is still unknown whether under homeostatic conditions the effect of the absence of Tregs is unique in BAMBI-KO mice.

For this purpose, we proposed the following objectives:

1. To evaluate whether epigenetic mechanisms are involved in the protection of BAMBI-KO mice against DSS-colitis.
2. To characterize the relevance of Treg cells in the protective phenotype observed in BAMBI-KO mice

5-Azacytidine Abrogates DSS-Colitis Resistance in BAMBI Deficient Mice

Research carried out by our group has shown that colon microbiota could participate in the protective effect against DSS-colitis in BAMBI-deficient mice. As changes in gene expression were observed in IECs, we proposed that colon microbiota induced epigenetic modifications in IECs of BAMBI-KO mice, contributing to protection against DSS-colitis.

WT and BAMBI-KO mice were treated with the epigenetic inhibitor 5-AZA, a DNA methylation inhibitor, 15 days prior to DSS exposure. Then, mice were monitored daily during the 8 days of DSS treatment to calculate the disease activity index (DAI) of each group. According to Figure 1A, the significant differences obtained between untreated WT and BAMBI-KO mice are not observed between WT and BAMBI-KO mice treated with 5-AZA. Thus, treated WT and BAMBI-KO mice show an intermediate phenotype with no exacerbated colitis symptoms, whereas untreated WT mice developed severe colitis, and untreated BAMBI-KO mice were protected from disease.

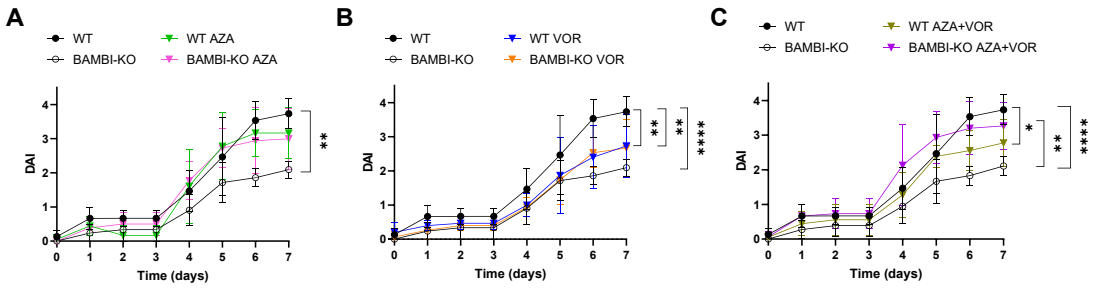

Figure 1. DAI scores of WT and BAMBI-KO mice treated with DSS.

B6 mice were administered 3% DSS in drinking water for 5 days, followed by 2 days of water. (**A**) 5-AZA group. The graph represents the DAI scores of WT and BAMBI-KO controls and WT and BAMBI-KO mice treated with 5-AZA. (**B**) VOR group. (**C**) 5-AZA + VOR group. The data shown are the mean ± SD. p values were calculated using Two - Way ANOVA test with Bonferroni correction, *p<0.05, **p<0.01. ***p<0.001, ****p<0.0001. ns=not significant.

These data support that DNA methylation processes in IECs regulate the development of DSS-colitis, considering that when 5-AZA was inoculated, either in the presence or absence of BAMBI, mice show alterations in DSS-susceptibility. Moreover, since the presence of microbiota is essential for the protection of BAMBI-KO mice, the impact of gut commensal can be mediated by epigenetic modifications which define a specific transcriptional program required to abrogate colitis development.

Vorinostat Treatment Eliminates the Protective Effect of BAMBI-KO Mice in DSS-Colitis model

Based on the impact of DNA methylation inhibitors, we aimed to further investigate other epigenetic modifications that could be involved in the protection against DSS-colitis. Therefore, WT and BAMBI-KO mice were treated with VOR, a histone deacetylation inhibitor. Similarly, mice received VOR injections during the 15 days preceding DSS-colitis induction and throughout the 7 days of DSS treatment mice were monitored to assess the DAI for each group.

As presented in Figure 1B, both WT and BAMBI-KO mice show a similar pattern when treated with VOR, as they showed after 5-AZA injection. Hence, under VOR treatment both groups exhibited nearly identical pathological features. By contrast, when VOR is not administered, the absence of BAMBI conferred resistance to DSS-colitis compared to WT mice.

These results suggest that, similar to DNA methylation, a specific histone deacetylation program is not only a key factor for DSS-colitis development but also for the protection against colitis observed in the absence of BAMBI.

Combined Epigenetic Therapy With 5-Azacytidine and Vorinostat Abolishes Colitis Protection in BAMBI Deficient Mice

Given that both 5-Azacytidine and Vorinostat monotherapy induced changes in the severity of DSS-colitis in WT and BAMBI-KO mice, we also wanted to investigate their combined effect. Therefore, both groups were treated with 5-AZA and VOR to determine whether the administration of both drugs could have an additive or a neutral interaction followed by DSS-colitis induction.

As observed in Figure 1C, treatment with 5-AZA and VOR synergically alters DSS-colitis in both WT and BAMBI-KO groups. Unlike the single therapy with either 5-AZA or VOR that exhibited intermediate phenotypes, the combined treatment can completely abrogate the protection against colitis in BAMBI-deficient mice, developing a more aggressive form of colitis than untreated BAMBI-KO mice. In contrast, WT mice treated with both inhibitors significantly decrease inflammation and show less colitis symptoms than untreated WT mice. These data correlate with histological tissue sections collected from distal colon samples of DSS-colitis mice. According to Figure 2, untreated WT mice showed a pronounced leukocytic infiltration in the lamina propria, a signal of inflammation, whereas untreated BAMBI-KO mice exhibited preserved colonic architecture. Likewise, mice treated with either AZA or VOR presented partial preservation of crypts and moderate leukocytic infiltration. Notably, BAMBI-KO mice treated with the combination therapy showed significant inflammatory activity, resembling the untreated WT group.

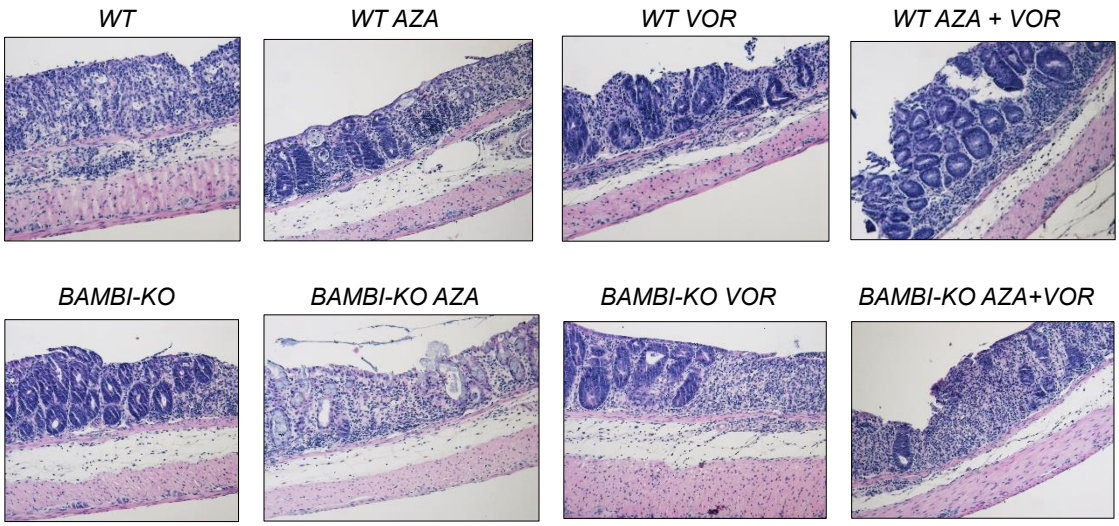

Figure 2. HE stains of distal colon samples after DSS-colitis induction.

WT and BAMBI-KO mice were given 3% DSS in drinking water for 5 days. On day 7, mice were sacrificed, and large intestine tissues were isolated, fixed in formaldehyde and embedded in paraffin for histological analysis.

Together these results highlight the relevance of the epigenetic program on intestinal inflammatory diseases. Once this program is totally abrogated by the inhibition of both DNA methylation and HDAC processes, WT mice show a better outcome when exposed to DSS. Interestingly, under these conditions, protection observed in the absence of BAMBI is completely abrogated defining an essential epigenetic program in the intestinal epithelium to develop DSS susceptibility. In addition, the microbiome-dependent mechanism of protection supports the relevance of intestinal microenvironment in this effect and further investigations will focus on the IECs which represent the physical connection between the gut commensal species and the immune populations and thereby are key regulators of intestinal inflammation.

Optimized protocol for Intestinal Epithelium Isolation and Purification

Due to the pivotal role of the epigenetic program in DSS-colitis model, we aimed to isolate the intestinal epithelium from full colon for further analysis of transcriptomic and metabolomic interactions that take place in this location during DSS-colitis induction in either presence of absence of BAMBI. Therefore, an IEp purification assay was carried out.

Once the epithelial layer of the colon was isolated from the whole tissue, purification was tested in samples of both full colon and isolated colon epithelium from WT mice by the analysis of the expression of E-cadherin and fibronectin via real-time quantitative reverse transcriptase polymerase chain reaction (RT-qPCR). Both proteins have important functions in cellular adhesion, cellular migration and tissular organization. E-cadherin is a calcium-dependent cell-cell adhesion protein located in the basolateral membrane of epithelial cells whereas fibronectin is an extracellular matrix protein located in the mesenchyme.[24] Therefore, E-cadherin is expressed in the IEp and fibronectin is only expressed in the mesenchyme.

According to Figure 3A, E-cadherin expressions were similar in full colon and epithelium. In contrast, the analysis of two types of fibronectins, fibronectin I and fibronectin II showed that this mesenchymal marker was only expressed in full colon. These data demonstrated a correct purification of the IEp with no mesenchymal contamination.

Moreover, since different T-cell and B-cell subpopulations can reside in the epithelium, we further determine the presence of these lymphocytes in our purified epithelium. The expression of CD3 and B220 markers was analyzed in full colon and in IEp by RT-qPCR to identify T-cells and B-cells infiltration respectively. The results showed that the expression of both markers in colon epithelium was very low compared to full colon (Figure 3B) defining very poor infiltration of immune cells after our process of epithelium purification.

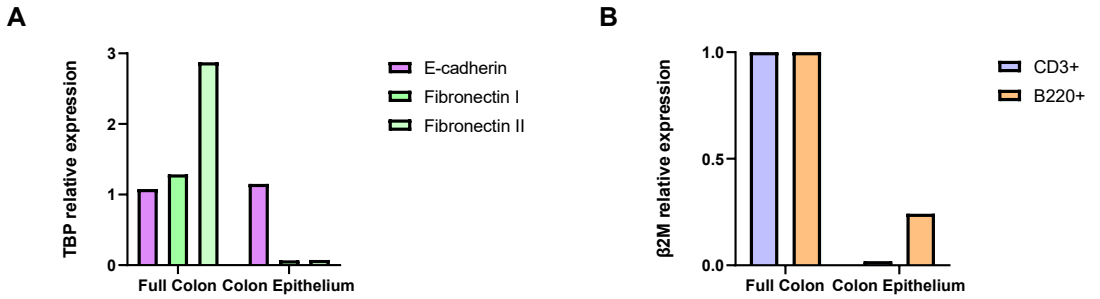

Figure 3. Assessment of the purity of intestinal epithelium samples.

(**A**) Expression of specific epithelial genes (E-cadherin) and specific mesenchymal genes (fibronectin) in full colon tissue and isolated IEp samples from WT mice were evaluated by RT-qPCR using SYBR Green technology. (**B**) Expression of immune markers CD3 (T lymphocytes) and B220 (B lymphocytes) in full colon tissue and isolated IEp samples from WT mice were assessed by RT-qPCR using TaqMan probes. Data shown are the mean normalized to the expression of the housekeeping gene TATA-box binding protein (TBP) and β2-microglobuline (β2M)

Selective Depletion of Treg cells generate distinctive cell distribution in the absence of BAMBI

Previous research carried out by our group using Treg depletion has shown that this population is essential for BAMBI-KO mice to be protected against inflammatory and autoimmune diseases, which is not observed in the DSS-colitis model. Thus, we have generated a spontaneous inflammatory disease mouse model by depleting Tregs to study whether the absence of BAMBI alters the distribution of peripheral lymphocytes.

The Treg-depleted mouse model was induced in WT and BAMBI-KO mice via diphtheria toxin (DTx) administration. DTx is a bacterial toxin that binds to the diphtheria toxin receptor (DTR) and induces cell death. Previous data demonstrated that murine cells are resistant to DTx because they lack the DTR. Genetically engineered mouse strains were developed by inserting the human DTR gene conjugated to green fluorescent protein (GFP) downstream of Foxp3 promoter. Thus, by injecting DTx into $Foxp3^{DTR}$ mice, the toxin depletes $Foxp3^{+}$ cells, including Treg cells.[25] To confirm effective depletion of Tregs upon DTx administration, we analyzed the expression of GFP by flow cytometry (Figure 4). We compared control $Foxp3^{DTR}$ mice, which exhibited a $GFP^{+}CD4^{+}$

Treg population, with mice treated with DTx, which showed a reduced number of $GFP^{+}CD4^{+}$ Treg cells, indicating efficient Treg depletion.

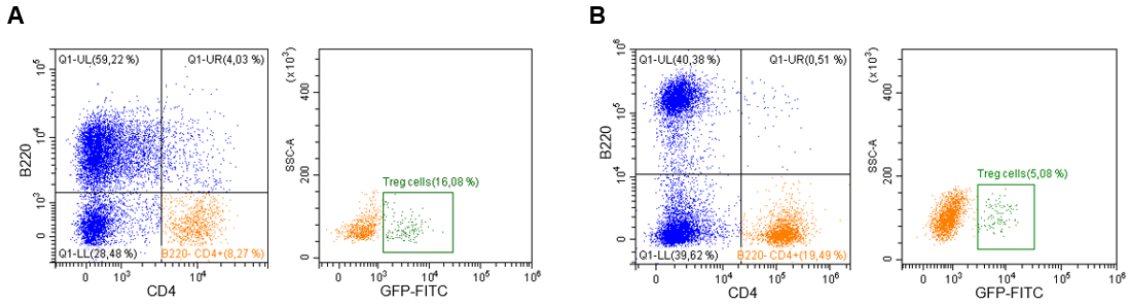

Figure 4. Gating strategy for the analysis of the depletion of Treg cells in Foxp3^{DTR} mice.

Representative flow cytometry plots showing the gating strategy followed to characterize Tregs in Foxp3^{DTR} mice. (**A**) Treg cells of control mice. (**B**) Treg cells after four weeks of DTx administration.

Considering the essential role of Tregs in the absence of BAMBI, we analyzed the abundance of other immune cell populations following Treg depletion. To that end, WT and BAMBI-KO spleen samples were collected after two and four weeks of DTx administration. Additionally, samples of untreated mice were also collected to serve as controls for comparation with treated groups. As observed in Figure 5, after DTx administration, both WT and BAMBI-KO mice, especially the WT group, exhibited a pronounced enlargement of the spleen, indicative of splenomegaly, typically associated with an autoimmune lymphoproliferative syndrome. In addition, both groups presented clearly visible cutaneous and ocular lesions, as well as behavioral changes associated with the syndrome.

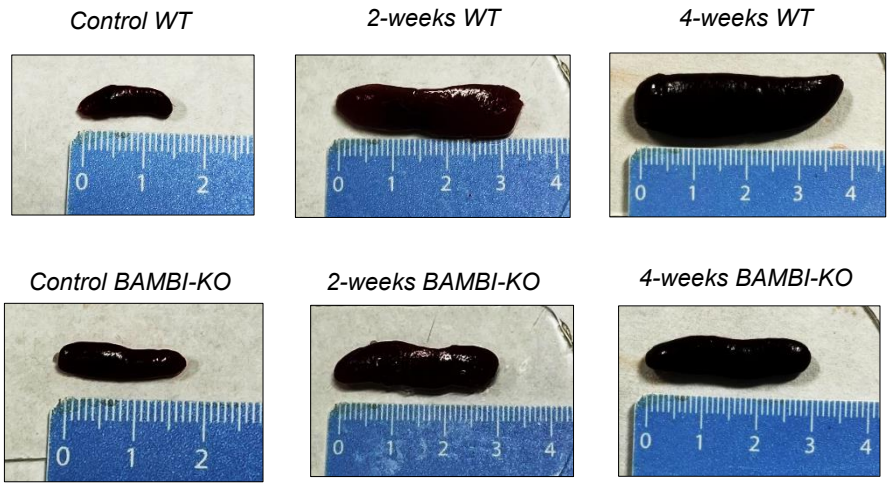

Figure 5. Representative images of spleens from WT and BAMBI-KO mice at different stages of DTx treatment.

Spleen sizes were captured in control mice, and after 2 and 4 weeks of DTx administration.

Upon analyzing different subpopulations of immune cells by flow cytometry, we observed that, in correlation with previous research by our group, BAMBI deficiency leads to an increased number of NK cells in homeostasis. Interestingly, the number of NK cells decreased after Treg depletion (Figure 6A), especially in mature NKs (Figure 6B). Nevertheless, this effect was not observed in WT mice, suggesting that Tregs, through the secretion of TGF-β, are the cells responsible for the proliferation of NKs in BAMBI-KO mice under physiological conditions.

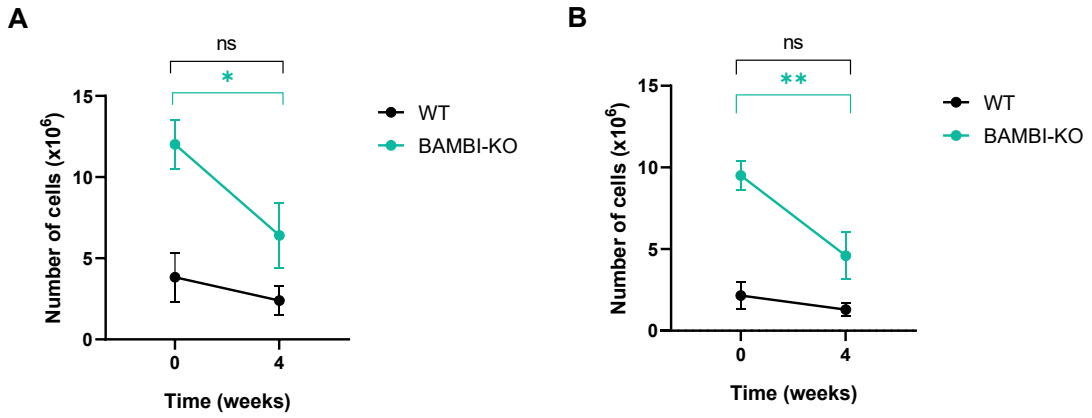

Figure 6. Number of NK cells in control and 4-week-treated WT and BAMBI-KO mice.

(**A**) Number of total NK cells. (**B**) Number of mature NK cells. The data shown are the mean ± SD. p values were calculated using Two - Way ANOVA test with Bonferroni correction, *p<0.05, **p<0.01. ***p<0.001, ****p<0.0001. ns=not significant.

Furthermore, T cell subpopulations were also analyzed (Figure S1). As expected, in the absence of a pivotal immuno-suppressive mechanism, naïve T cells were significantly reduced in both WT and BAMBI-KO mice (Figure S1C and D). Interestingly, we also observed an increased $CD8^+$ T cell population only in WT mice (Figure S1A). These differences can be explained by the increment of CD8 memory T cells, which are the only subpopulations that show divergent dynamic between WT and BAMBI-KO mice (Figure S1E and G). Together, these data show that BAMBI can modulate the tolerance induced by Tregs via TFG-β signaling. Further experiments will be required to elucidate whether this regulation is based on the Smad-dependent or independent pathways and the implication of other immune cells populations.

DISCUSSION

BAMBI is a transmembrane protein that controls TGF-β signaling. Previous studies have demonstrated that the absence of BAMBI enhances the differentiation of Treg cells and reduces the differentiation of Th17 cells, leading to protection against autoimmune diseases. In fact, a monoclonal antibody targeting BAMBI has been developed, showing enormous therapeutical potential in the protection against autoimmune inflammatory diseases including psoriasis and psoriatic arthritis via TGF-β dependent mechanisms.[13]

Based on these results, our laboratory group aimed to investigate the role of BAMBI in other autoimmune and chronic inflammatory diseases such as ulcerative colitis. After DSS administration, BAMBI-KO mice showed significantly less susceptibility to develop colitis than WT mice. Unlike other pathologies, this protection against DSS-colitis in BAMBI-KO mice was not mediated by Tregs. Interestingly, this effect was microbiome-dependent since under SPF conditions BAMBI-KO mice were not protected against disease. The lack of immune-mediated suppressive mechanisms suggests a key role of the intestinal epithelium, where an alternative tolerogenic context influenced by gut microbiota is responsible for colitis protection.

Previous studies have investigated the relationship between microbiota and epigenetic mechanisms, and there is strong evidence that epigenetic modifications can be modulated by environmental factors such as microbiota.[26,27] The gut commensal can participate in the regulation of host immune response and homeostasis. This fact can be explained by the interaction between host cells and microbially metabolites such as short-chain fatty acids (SCFAs), tryptophan (Trp) and bile acid (BA) metabolites.[28]

To test whether the epigenetic modifications would be involved in the genetic program required to provide resistance to DSS, we employed two epigenetic inhibitors: 5-Azacytidine, a DNA methyltransferase inhibitor, and Vorinostat, a HDAC inhibitor. Both drugs have been approved by the FDA and are currently used in cancer therapy. 5-AZA has been approved for the treatment of myelodysplastic syndromes while Vorinostat has been approved for cutaneous T-cell lymphoma.[29] Furthermore, He *et al*., 2021 have studied the implication of Vorinostat in DSS-induced colitis with the aim of identifying synergistic drugs for 5-aminosalicylic (5-ASA), which is the first treatment option for UC. Although they focused on the combination treatment, they also obtained lower DAI values after Vorinostat treatment.[30]

In the present study, we used both inhibitors in DSS-induced colitis and results showed that WT mice treated with 5-AZA and Vorinostat, and especially the combination of both drugs, gained protection against DSS-colitis. On the contrary, treated BAMBI-KO mice lost protection against disease. Our findings support the initial hypothesis that protection in BAMBI-deficient mice was mediated by epigenetic mechanisms like DNA methylation and HDAC in IECs cells. Moreover, we demonstrated that the combined therapy has a synergistic effect, completely abrogating the protection in BAMBI-KO mice. Our data suggests that a defined epigenetic program, which includes DNA methylation and HDAC, is required to confer protection against DSS-colitis in BAMBI-deficient mice, and deficiency of this protection is more pronounced when both inhibitors are administered together. In conclusion, we state that colon microbiota acts differently over colon WT and BAMBI-KO IECs, programming a disease protective genetic profile in the absence of BAMBI. Therefore, the protection against DSS-colitis in BAMBI-deficient mice depends not only on the presence of gut microbiota but also on its capacity to modulate epigenetic programs within IECs.

Additionally, given that the intestinal epithelium plays a crucial role in IBDs, our group has previously performed IEp permeability assays and results showed that the colonic epithelium of BAMBI-KO mice was more resistant and less permeable than WT mice, which correlates with the protection against colitis in the absence of BAMBI. We have seen that WT mice present damages in the IEp after DSS exposure, and ongoing studies are evaluating whether adhesion or proapoptotic molecules could be involved. In the current work, we optimized the protocol for the isolation and purification of the IEp and demonstrated that our IEp samples express E-cadherin but not fibronectin, which is indicative of no mesenchymal contamination.[31] Moreover, we confirmed that the isolated epithelial sample is free from infiltrating lymphoid cells. This is the initial step to perform the required experiments to compare DNA and mRNA of intestinal epithelium between WT and BAMBI-KO mice.

Our laboratory group has demonstrated that, under pathological conditions, BAMBI-KO mice showed reduced levels of inflammation compared to WT mice. However, under homeostatic conditions, BAMBI-deficient mice exhibited increased proliferation of T and B lymphocytes, as well as NK cells which also showed enhanced cytotoxic activity (unpublished data). This paradoxical observation could be explained by the tolerogenic function of Tregs which, under pathological conditions, have demonstrated to be essential for generating protection.[32] Therefore, we aimed to further investigate the underlying protective mechanisms by depleting Tregs under homeostatic conditions.

Upon analyzing different immune cell subpopulations of NK, T and B cells, in control and Treg-depleted mice, we observed that BAMBI-KO mice had an increased number of NK cells at homeostasis while Treg depletion markedly reduced the number of NKs. Although previous studies have described TGF-β as a negative regulator of NK cell differentiation and activity,[33] our group has found that BAMBI deficiency promotes NK cell differentiation under homeostatic conditions. In this study, we confirmed the expansion of NKs observed in BAMBI-KO at homeostasis, and we noted that the number of NK cells, especially mature NKs, is reduced following Treg depletion. These data suggest that, in the absence of BAMBI, Tregs, via TGF-β secretion, which plays the pivotal role in the protection in autoimmune diseases, are conversely responsible for maintaining the elevated NK cell number under homeostatic conditions. This paradoxical effect could be explained by the dual role of TGF-β which can promote pro-inflammatory or anti-inflammatory responses according to the cytokine environment.[34]

In conclusion, our results reveal a complex interplay between BAMBI, Tregs and NK cells. These findings contribute to a deeper understanding of the regulatory mechanisms that control the immune response in the absence of BAMBI and highlight potential therapeutic strategies targeting NK cell responses.

METHODS

Animals

C57BL/6 WT mice were obtained from Charles River (Wilmington, Massachusetts; USA). 129SvJ/B6 BAMBI-KO mice were generated following the description of Tramullas and collaborators.[35] BAMBI-KO mice were then crossed with C57BL/6 WT mice for up to twelve generations. Crossbreeding of BAMBI$^{+/-}$ mice generated homozygous mutants. B6/Foxp3^{DTR} WT and B6/Foxp3^{DTR} BAMBI-KO mice have been generated in our laboratory. Mouse genotyping was confirmed by PCR from tail DNA.

All *in vivo* studies have been approved by the Institutional Committee for the Care and Use of Laboratory Animals of the University of Cantabria and carried out in accordance with the Declaration of Helsinki and the Directive of the Council of the European Communities (86/609/EEC).

Preparation of mice for DSS-colitis

To characterize the role of epigenetic modifications in the protection against DSS-induced colitis, male mice aged two to three months were used. WT and BAMBI-KO mice were housed in a conventional animal facility and kept in co-housing for 15 days prior to disease induction. Each genotype group (WT and BAMBI-KO) was divided into four subgroups: control, 5-AZA-treated, Vorinostat-treated and combination-treated (5-AZA + Vorinostat).

Mice in the 5-AZA group received intraperitoneal injections of 50 µg of 5-AZA (Sigma) twice per week, while mice in the Vorinostat group received daily intraperitoneal injections of 50 mg/kg/day of Vorinostat (Selleck Chem). These treatments were designed to inhibit DNA methylation and histone deacetylase activity, respectively.

Induction and evaluation of DSS-colitis in mice

For colitis induction, DSS (36,000-50,000 M.Wt., MP Biomedicals) was dissolved in water at a concentration of 3%. Mice received the DSS solution via drinking water, which was refreshed daily. Treatment continued until animals in the control group reached a DAI between 1.5 and 2, typically within 4 to 5 days.

The DAI was calculated daily based on three clinical parameters: A) Weight loss: scored as 0 (no weight loss), 1 (1–5% weight loss), 2 (5–10% weight loss), 3 (10–20% weight loss), and 4 (>20% weight loss); stool: scored as 0 (normal consistency stool), 2 (loose stool), and 4 (diarrhea); C) Rectal bleeding: scored as 0 (no bleeding), 2 (light bleeding), and 4 (heavy bleeding). The final DAI score was calculated as the average of the three individual scores.

On the initial day of DSS administration, mice were weighed, and fecal and blood samples were collected for metabolomic studies and plasma extraction. Mice were sacrificed on day 7. Fecal and plasma samples were also collected. In addition, large intestine tissues were isolated, fixed in formaldehyde and embedded in paraffin for histological analysis. The volume of DSS-treated water remaining in each cage was measured daily. Mice exhibiting body weight loss greater than 25% of their initial weight were euthanized in accordance with institutional animal welfare guidelines.

Intestinal epithelium purification

B6 mice from the conventional animal room facility have been euthanized to obtain the colon intestine. Firstly, 4-5 cm long intestine fragments were washed in cold PBS. Then, the digestive tube was inverted with the aid of a serrated steel needle and a surgical suture, hence, the IE was in the outside while the muscle layer stayed on the inside of the needle. Next, samples were washed again with cold PBS to remove tissue remnants followed by incubation in a tube with isolation solution (BD Cell Recovery Solution; BD Biosciences) for 20 minutes on ice, shaking every 5 minutes. During the incubation, the intestinal basement membrane was dissolved, and the IE was released from the mesenchyme. IE was transferred to an Eppendorf tube and incubated for 2 minutes at 37°C with trypsin solution at 2.5 mg/ml.

RNA extraction, cDNA synthesis and expression analysis by RT-qPCR

To confirm that the sample isolated from the intestine was indeed intestinal epithelium, a RT-qPCR comparing the expression of E-cadherin and fibronectin was carried out. First, under sterile conditions, intestinal samples were transferred to Eppendorf tubes of 2 mL. 400 µL of TRIzol Reagent (Invitrogen) were added and tissue was homogenized. This step was repeated twice. Next, samples were centrifuged at 1300 revolutions per minute (rpm) for 0.5 minutes at 4 °C. 600 µL of supernatant were placed into another Eppendorf tube and the same volume of ethanol (maximum purity) was added. Then, total RNA was extracted from the tissue using the RNA Purification Zymo Research Kit (Direct-zol RNA miniprep; Cat. No: R2052) following the manufacturer's instructions and RNA concentration and purity were measured using a spectrophotometer (Nanodrop 2000, Thermo Scientific).

1 µg RNA was converted into 1 µg cDNA by reverse transcription using the iScript cDNA Synthesis Kit (Bio-Rad) following the manufacturer's protocol. The mix was amplified in a thermocycler (2720 Thermal cycler, Applied Biosystems) following the protocol: 5'-25ºC, 20'-46ºC, 1'-95ºC and hold at 4ºC.

qPCR was performed using the PowerUp SYBR Green Master Mix (Thermo Fisher Scientific, UK). Specific primers were employed for the amplification of the genes (Table S1A). Each reaction was run in triplicate in a total reaction volume per well of 25 µL containing 12.5 µL of Syber green master mix, 1.75 µL of forward primer [10 nmol], 1.75 µL of reverse primer [10 nmol], 6 µL of H_2O and 9 µL of cDNA (diluted 1:5). Results were analyzed using *StepOne Software* by the ΔΔCt method and normalized to levels of TBP.

cDNA was also employed to analyze the expression of T and B lymphocytes in total colon and IEp. qPCR was performed using TaqMan Gene Expression Assays (Applied Biosystems). Specific TaqMan probes (Table S1B) conjugated to FAM fluorochrome (Applied Biosystems) were used for the expression of CD3 and B220 markers. Each reaction was run in triplicate in a total reaction volume per well of 20 µL containing 10 µL of TaqMan master mix, 1 µL of 20X probe, 5 µL of H_2O and 4 µL of cDNA. Results were analyzed using *StepOne Software* by the ΔΔCt method and normalized to levels of β2-microglobuline.

Induction of Treg depleted mouse model

To analyze the surveillance and the different cell populations of Treg depleted WT and BAMBI-KO mice, B6/Foxp3^{DTR} male mice aged two to three months were employed. All mice were housed in a conventional animal facility. WT and BAMBI-KO mice received

intraperitoneal injections of DTx (Sigma-Aldrich) at a dose of 0.5 µg per mouse thrice per week during the first week of treatment and twice per week during the following weeks of treatment. DTx was diluted in sterile phosphate buffered saline (PBS) and aliquots were stored at -80ºC.

Spleen extraction and sample preparation

B6/Foxp3^{DTR} mice were euthanized for spleen collection. Spleen samples were weighted and measured. The procedure was performed under conditions of maximal sterility as possible. 15 mL falcon tubes containing 2 mL PBS were used to place the spleens, remaining on ice until processing. The spleens were placed in petri dishes and mechanically disaggregated using the plunger of a sterile syringe and washed with 2 mL of PBS. The resulting cell suspension was transferred to new falcon tubes, followed by centrifugation at 1500 rpm for 5 minutes at 4 °C. The supernatant was discarded, and the cell pellet was resuspended in 3 mL of red blood cell (RBC) lysis buffer per spleen. The lysis buffer consisted of 9 parts of Buffer II (0.89 g of NH_4Cl in 100 mL of H_2O) and 1 part of Buffer I (2.06 g of Tris in 100 mL of H_2O). The suspension was incubated at room temperature for 7 minutes. After incubation, cells were washed with 10 mL of PBS and centrifuged at 1500 rpm for 5 minutes at 4 °C. The supernatant was discarded, and the washing step was repeated. Finally, the cell pellet was resuspended in 10 mL of PBS. Cell counting was performed using Countess 3 automated counter, Thermo Fisher Scientific (Waltham, Massachusetts; USA).

Characterization of Spleen NK cell, T cell and B cell populations

Cell populations were analyzed by flow cytometry using CytoFLEX (Beckman Coulter Life Sciences, Indianapolis, IN, USA). Firstly, cytometer tubes were filled with $2x10^6$ spleen cells from each WT or BAMBI-KO sample. Then, 50 µL from pools 1-6 were added to the corresponding tubes. Each pool contained PBS, normal rat serum (NRS), anti-FcγRII to block Fc receptors and a mix of antibodies conjugated to different fluorochromes. The fluorochromes used were (Table S2): FITC (fluorescein isothiocyanate), PE (phycoerythrin), PE-Cy7 (phycoerythrin-cyanine-y-7), APC (allophycocyanin), PerCP-Cγ5 (peridin-chlorophyll-cyanine-γ-5), APC-Cγ7 (allophycocyanin-cyanine-γ-7) and PB (Pacific blue). Next, tubes were incubated at 4°C in darkness for 20 minutes. After the primary staining of pools 1, 4 and 5, a second incubation step was required due to the presence of biotin-conjugated antibodies. Later, cells were washed with 2 mL of PBS and centrifuged at 1500 rpm for 5 minutes at 4°C. Finally, the supernatant was discarded and 200 µL of PBS were added to each tube. The different cell populations were analyzed using the software *CytExpert* version *2.5.* according to the expression profile of the markers.

Gating strategy

Spleen NK cells, T lymphocytes, B lymphocytes and their different cell subpopulations were compared between WT and BAMBI-KO mice by flow cytometry, using the *CytExpert* program. The gating strategy used to analyze the cell populations is shown in Figure S2. First, P1 was limited by excluding possible doublets, which are aggregated cells that could be detected as a single cell in the flow cytometer. Doublets were excluded according to their weight (FSC-H) and area (FC-A). Then, according to its size (FSC, Forward Scatter) and complexity (SSC, Side Scatter), the area of the lymphocyte population (P2) was selected. The P2 gate was subsequently expanded to include blasts. Beyond this point, specific markers were used to identify the different cell populations.

NK cells were first selected from cells that did not express CD3 marker. From this population, NK1.1^{+}CD49b^{+} cells were selected for the analysis of the different subpopulations of NK cells. Immature NK cells expressed the markers CD27^{+}CD11b^{-}, transitional cells CD27^{+}CD11b^{+}, and mature NK cells CD27^{-}CD11b^{+}.

In contrast, T lymphocytes were selected from P2 cells that express CD3 marker. Then, from this population, CD4^{+} and CD8^{+} T cells were selected according to their respective markers. Finally, for the analysis of T memory cells, CD4^{+} and CD8^{+} cell subpopulations of each group were analyzed. Effector memory had a CD62L^{-}CD44^{+} phenotype, central memory CD62L^{+}CD44^{+}; and naïve T cells CD62L^{+}CD44^{-}. In addition to this, we also analyzed Treg cells, which had a B220^{-}CD4^{+} phenotype.

B lymphocytes were selected from P2 cells that express B220 marker. Next, different receptors and ligands (IgM^{+}, IgD^{+}, ICOSL^{+}, BAFFR^{+}) were analyzed from B220^{+} cells to compare their different expression and fluorescence between WT and BAMBI-KO mice. Furthermore, we followed two different gating strategies to analyze Bregs. One approach was to select P2 cells that expressed CD19 marker. Then, Bregs were identified by the following phenotype, CD23^{high}CD1d^{high}CD21^{high} IgM^{+}IgD^{+}. Alternatively, we also selected Bregs from P2 cells that expressed B220 marker, followed by the expression of IgM^{+}CD5^{+}CD1d^{high}.

Statistical analysis

Graphs and statistical analysis have been made using the software *GraphPad Prism* version *8.0*. Significant differences were considered as no significant p≥0,05 (ns); significant p< 0.05 (*); very significant p< 0.01 (**); strongly significant p< 0.001 (***) and highly significant p< 0.0001 (****).

In DSS-induced colitis experiment, it has been used Two-Way ANOVA test to compare the final DAI score of the different WT and BAMBI-KO subgroups. To compare the different cell subpopulations in Treg depleted mice, Two-Way ANOVA test was also employed. Multiple comparations were adjusted using the Bonferroni correction.

AGRADECIMIENTOS

Mi primer agradecimiento es para mis directores, Ramón y Luis, por su cercanía y apoyo constante, dedicándome su tiempo, sus conocimientos y su experiencia a lo largo de este proceso.

También quiero dar las gracias a Fernando e Iván, por su ayuda continua y por crear un ambiente tan agradable en el laboratorio; a David y a Patricia por su trabajo siempre eficaz y a los miembros de Inhibitec, por su paciencia y por estar siempre dispuestos a enseñarme nuevas técnicas, compartiendo sus conocimientos conmigo.

Por último, quiero agradecer a mis padres, a Rodrigo y a mis amigos su apoyo incondicional en esta etapa tan especial de mi vida. Me han acompañado en los momentos difíciles y han celebrado conmigo cada pequeño logro.

REFERENCES

1. Tomar, N., and De, R.K. (2014). A brief outline of the immune system. Methods Mol. Biol. Clifton NJ 1184, 3–12. https://doi.org/10.1007/978-1-4939-1115-8_1.

2. Mancini, M., and Vidal, S.M. (2020). Mechanisms of Natural Killer Cell Evasion Through Viral Adaptation. Annu. Rev. Immunol. 38, 511–539. https://doi.org/10.1146/annurev-immunol-082619-124440.

3. LeBien, T.W., and Tedder, T.F. (2008). B lymphocytes: how they develop and function. Blood 112, 1570–1580. https://doi.org/10.1182/blood-2008-02-078071.

4. Lees, J.R. (2020). CD8+ T cells: The past and future of immune regulation. Cell. Immunol. 357, 104212. https://doi.org/10.1016/j.cellimm.2020.104212.

5. Dong, C. (2021). Cytokine Regulation and Function in T Cells. Annu. Rev. Immunol. 39, 51–76. https://doi.org/10.1146/annurev-immunol-061020-053702.

6. Sallusto, F., Geginat, J., and Lanzavecchia, A. (2004). Central memory and effector memory T cell subsets: function, generation, and maintenance. Annu. Rev. Immunol. 22, 745–763. https://doi.org/10.1146/annurev.immunol.22.012703.104702.

7. Lee, G.R. (2018). The Balance of Th17 versus Treg Cells in Autoimmunity. Int. J. Mol. Sci. 19, 730. https://doi.org/10.3390/ijms19030730.

8. Georgiev, P., Charbonnier, L.-M., and Chatila, T.A. (2019). Regulatory T Cells: The Many Faces of Foxp3. J. Clin. Immunol. 39, 623–640. https://doi.org/10.1007/s10875-019-00684-7.

9. Syed, V. (2016). TGF-β Signaling in Cancer. J. Cell. Biochem. 117, 1279–1287. https://doi.org/10.1002/jcb.25496.

10. Bettelli, E., Carrier, Y., Gao, W., Korn, T., Strom, T.B., Oukka, M., Weiner, H.L., and Kuchroo, V.K. (2006). Reciprocal developmental pathways for the generation of pathogenic effector TH17 and regulatory T cells. Nature 441, 235–238. https://doi.org/10.1038/nature04753.

11. Mucida, D., Park, Y., Kim, G., Turovskaya, O., Scott, I., Kronenberg, M., and Cheroutre, H. (2007). Reciprocal TH17 and regulatory T cell differentiation mediated by retinoic acid. Science 317, 256–260. https://doi.org/10.1126/science.1145697.

12. Chen, X., Li, J., Xiang, A., Guan, H., Su, P., Zhang, L., Zhang, D., and Yu, Q. (2024). BMP and activin receptor membrane bound inhibitor: BAMBI has multiple roles in gene expression and diseases (Review). Exp. Ther. Med. 27, 28. https://doi.org/10.3892/etm.2023.12316.

13. Postigo, J., Iglesias, M., Álvarez, P., Jesús Augustin, J., Buelta, L., Merino, J., and Merino, R. (2016). Bone Morphogenetic Protein and Activin Membrane-Bound Inhibitor, a Transforming Growth Factor β Rheostat That Controls Murine Treg Cell/Th17 Cell Differentiation and the Development of Autoimmune Arthritis by Reducing Interleukin-2 Signaling. Arthritis Rheumatol. Hoboken NJ 68, 1551–1562. https://doi.org/10.1002/art.39557.

14. Augustín, J.J., Alvarez, P., Tamayo, E., Iglesias, M., Merino, J., and Merino, R. (2017). BAMBI is a negative regulator of humoral immune responses. J. Immunol. 198, 152.13. https://doi.org/10.4049/jimmunol.198.Supp.152.13.

15. Seyedian, S.S., Nokhostin, F., and Malamir, M.D. (2019). A review of the diagnosis, prevention, and treatment methods of inflammatory bowel disease. J. Med. Life 12, 113–122. https://doi.org/10.25122/jml-2018-0075.

16. Sáiz-Chumillas, R.M., Barrio, J., Fernández-Salazar, L., Arias, L., Sierra Ausín, M., Piñero, C., Fuentes Coronel, A., Mata, L., Vásquez, M., Carbajo, A., et al. (2023). Incidencia e historia natural de la enfermedad inflamatoria intestinal en Castilla y León: estudio prospectivo, multicéntrico y poblacional. Gastroenterol. Hepatol. 46, 102–108. https://doi.org/10.1016/j.gastrohep.2022.04.002.

17. Wangchuk, P., Yeshi, K., and Loukas, A. (2024). Ulcerative colitis: clinical biomarkers, therapeutic targets, and emerging treatments. Trends Pharmacol. Sci. 45, 892–903. https://doi.org/10.1016/j.tips.2024.08.003.

18. Shi, N., Li, N., Duan, X., and Niu, H. (2017). Interaction between the gut microbiome and mucosal immune system. Mil. Med. Res. 4, 14. https://doi.org/10.1186/s40779-017-0122-9.

19. Wiertsema, S.P., van Bergenhenegouwen, J., Garssen, J., and Knippels, L.M.J. (2021). The Interplay between the Gut Microbiome and the Immune System in the Context of Infectious Diseases throughout Life and the Role of Nutrition in Optimizing Treatment Strategies. Nutrients 13, 886. https://doi.org/10.3390/nu13030886.

20. Konkel, J.E., and Chen, W. (2011). Balancing acts: the role of TGF-β in the mucosal immune system. Trends Mol. Med. 17, 668–676. https://doi.org/10.1016/j.molmed.2011.07.002.

21. Vlantis, K., Polykratis, A., Welz, P.-S., van Loo, G., Pasparakis, M., and Wullaert, A. (2016). TLR-independent anti-inflammatory function of intestinal epithelial TRAF6 signalling prevents DSS-induced colitis in mice. Gut 65, 935–943. https://doi.org/10.1136/gutjnl-2014-308323.

22. Krawczyk, J., Keane, N., Freeman, C.L., Swords, R., O'Dwyer, M., and Giles, F.J. (2013). 5-Azacytidine for the treatment of myelodysplastic syndromes. Expert Opin. Pharmacother. 14, 1255–1268. https://doi.org/10.1517/14656566.2013.794222.

23. Nguyen, T.T.T., Zhang, Y., Shang, E., Shu, C., Torrini, C., Zhao, J., Bianchetti, E., Mela, A., Humala, N., Mahajan, A., et al. (2020). HDAC inhibitors elicit metabolic reprogramming by targeting super-enhancers in glioblastoma models. J. Clin. Invest. 130, 3699–3716. https://doi.org/10.1172/JCI129049.

24. Sarpdag, F., Yönem, O., Aktas, A., Seckin, Y., Tuncer, E., and Ozer, H. (2021). Colonic fibronectin and E-cadherin in mild ulcerative colitis. Bratisl. Lek. Listy 122, 331–335. https://doi.org/10.4149/BLL_2021_056.

25. Chapman, T.J., and Georas, S.N. (2013). Adjuvant effect of diphtheria toxin after mucosal administration in both wild type and diphtheria toxin receptor engineered mouse strains. J. Immunol. Methods 400–401, 122–126. https://doi.org/10.1016/j.jim.2013.10.010.

26. Cuevas-Sierra, A., Ramos-Lopez, O., Riezu-Boj, J.I., Milagro, F.I., and Martinez, J.A. (2019). Diet, Gut Microbiota, and Obesity: Links with Host Genetics and Epigenetics and Potential Applications. Adv. Nutr. Bethesda Md 10, S17–S30. https://doi.org/10.1093/advances/nmy078.

27. Mostafavi Abdolmaleky, H., and Zhou, J.-R. (2024). Gut Microbiota Dysbiosis, Oxidative Stress, Inflammation, and Epigenetic Alterations in Metabolic Diseases. Antioxid. Basel Switz. 13, 985. https://doi.org/10.3390/antiox13080985.

28. Wang, J., Zhu, N., Su, X., Gao, Y., and Yang, R. (2023). Gut-Microbiota-Derived Metabolites Maintain Gut and Systemic Immune Homeostasis. Cells 12, 793. https://doi.org/10.3390/cells12050793.

29. Di Costanzo, A., Del Gaudio, N., Migliaccio, A., and Altucci, L. (2014). Epigenetic drugs against cancer: an evolving landscape. Arch. Toxicol. 88, 1651–1668. https://doi.org/10.1007/s00204-014-1315-6.

30. He, L., Wen, S., Zhong, Z., Weng, S., Jiang, Q., Mi, H., and Liu, F. (2021). The Synergistic Effects of 5-Aminosalicylic Acid and Vorinostat in the Treatment of Ulcerative Colitis. Front. Pharmacol. 12, 625543. https://doi.org/10.3389/fphar.2021.625543.

31. Griggs, L.A., and Lemmon, C.A. (2023). Spatial Gradients of E-Cadherin and Fibronectin in TGF-β1-Treated Epithelial Colonies Are Independent of Fibronectin Fibril Assembly. Int. J. Mol. Sci. 24, 6679. https://doi.org/10.3390/ijms24076679.

32. Sakaguchi, S., Yamaguchi, T., Nomura, T., and Ono, M. (2008). Regulatory T cells and immune tolerance. Cell 133, 775–787. https://doi.org/10.1016/j.cell.2008.05.009.

33. Regis, S., Dondero, A., Caliendo, F., Bottino, C., and Castriconi, R. (2020). NK Cell Function Regulation by TGF-β-Induced Epigenetic Mechanisms. Front. Immunol. 11, 311. https://doi.org/10.3389/fimmu.2020.00311.

34. Wang, J., Zhao, X., and Wan, Y.Y. (2023). Intricacies of TGF-β signaling in Treg and Th17 cell biology. Cell. Mol. Immunol. 20, 1002–1022. https://doi.org/10.1038/s41423-023-01036-7.

35. Tramullas, M., Lantero, A., Díaz, A., Morchón, N., Merino, D., Villar, A., Buscher, D., Merino, R., Hurlé, J.M., Izpisúa-Belmonte, J.C., et al. (2010). BAMBI (bone morphogenetic protein and activin membrane-bound inhibitor) reveals the involvement of the transforming growth factor-beta family in pain modulation. J. Neurosci. Off. J. Soc. Neurosci. 30, 1502–1511. https://doi.org/10.1523/JNEUROSCI.2584-09.2010.

Trabajo de Fin de Grado
Grado en Ciencias Biomédicas · Facultad de Medicina
2024 – 2025

Supplemental information

The role of BAMBI in TGF-β signaling during homeostasis and inflammation

Paula Bermúdez Revuelta[1], Ramón Merino Pérez[2], Luis Gil de Gómez Sesma[1]

UC | Universidad de Cantabria

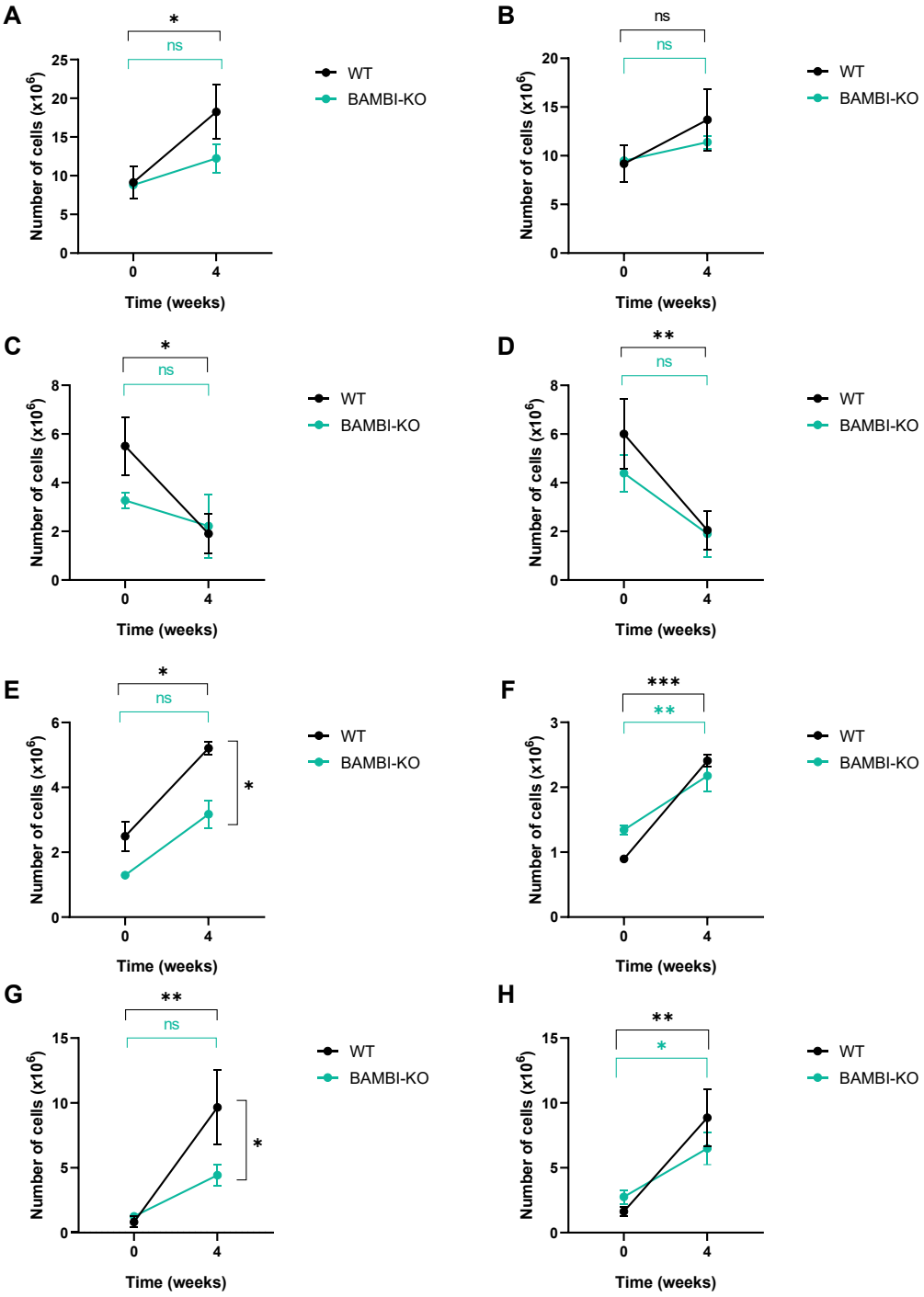

Figure S1. Number of T cells in control and 4-week-treated WT and BAMBI-KO mice.

(**A**) Number of CD8⁺ T cells. (**B**) Number of CD4⁺ T cells. (**C**) Number of naïve CD8⁺ T cells. (**D**) Number of naïve CD4⁺ T cells. (**E**) Number of CD8⁺ Tcm cells. (**F**) Number of CD4⁺ Tcm cells. (**G**) Number of CD8⁺ Tem cells. (**H**) Number of CD4⁺ Tem cells. The data shown are the mean ± SD. p values were calculated using Two - Way ANOVA test and Bonferroni correction, *p<0.05, **p<0.01. ***p<0.001, ****p<0.0001. ns=not significant.

A

Gene	Sequence
E-cadherin	Fwd: 5'-CTGCTGCTCCTACTGTTTC-3' Rev: 5'-CTGGCTCAAATCAAAGTCC-3'
Fibronectin I	Fwd: 5'-ACATCACTGGGGGTGTGGATT-3' Rev: 5'-GCTGTGACAACTGCCGTAGA-3'
Fibronectin II	Fwd: 5'-GCCACTCTGACTGGCCTTAC-3' Rev: 5'- CCGTGTAAGGGTCAAAGCAT-3'
TBP	Fwd: 5'-CAAACCCAGAATTGTTCTCCTT-3' Rev: 5'-ATGTGGTCTTCCTGAATCCCT-3'

B

Gene	TaqMan Assay Reference (Applied Biosystems)
CD3 (CD247)	Mm.PT.58.41689106
B220	Mm.PT.58.7583849
β2-microglobuline	Mm.PT.39a.22214835

Table S1. Primer and probe information used for RT-qPCR.

(**A**) Sequences of the different primers used in gene expression studies with SYBR Green Mix. Primers were purchased from Invitrogen. (**B**) List of genes and corresponding TaqMan probes obtained from the Applied Biosystems assay library.

Murine Antibodies	Isotype	Clone	Fluorochrome	Pool	Laboratory
Anti-NK1.1	Rat IgG2 a,κ	PK136	PerCP-Cy5	1	BioLegend
Anti-CD3e	Armenian Hamster IgG	145-c11	Biotin	1	BD Bioscience
Anti-CD49b	Rat IgM κ	DX5	PB	1	BioLegend
Anti-CD11b	Rat IgG2 b,κ	M1/70	PE	1	BioLegend
Anti-CD27	Armenian Hamster IgG	LG.3A10	APC	1	BioLegend
Streptavidin			APC Cy7	1b	BioLegend
Anti-CD4	Rat IgG2 b,κ	GK 1,5	PB	2	BioLegend
Anti-CD8	Rat IgG2 a,κ	GK 1,5	PE Cy7	2	BioLegend
Anti-CD3e	Rat IgG2 b,κ	17A2	PerCP-Cy5	2	BioLegend
Anti-CD44	Rat IgG2 b,κ	IM7	PE	2	BioLegend
Anti-CD62L	Rat IgG2 a,κ	MEL-14	APC	2	BioLegend
Anti-B220	Rat IgG2 a,κ	RA3-6B2	PerCP-Cy5	3	BioLegend
Anti-ICOSL	Rat IgG2 a,κ	HK5.3	PE	3	BioLegend
Anti-BAFFR	Rat IgG1 κ	7H22-E16	APC	3	BioLegend
Anti-IgM	Rat IgG2 a,κ	RMM-1	APC-Cy7	3	BioLegend
Anti-IgD	Rat IgG2 a,κ	11-26c2a	PB	3	BioLegend
Anti-CD19	Rat IgG2 a,κ	6D5	APC	4	BioLegend
Anti-CD23	Rat IgG2 a,κ	B3B4	PE	4	BioLegend
Anti-IgM	Rat IgG2 a,κ	RMM-1	APC-Cy7	4	BioLegend
Anti-CD1d	Rat IgG2 b,κ	1B1	Biotin	4	Pharmigen
Anti-CD21	Rat IgG2 a,κ	7E9	PB	4	BioLegend
Anti-IgD	Rat IgG2 a,κ	11262a	FITC	4	Southern Bio
Streptavidin			PerCP-Cy5	4b	BD Bioscience
Anti-IgM	Rat IgG2 a,κ	RMM-1	APC-Cy7	5	BioLegend
Anti-CD1d	Rat IgG2 b,κ	1B1	Biotin	5	Pharmigen
Anti-B220	Rat IgG2 a,κ	RA3-gB2	APC	5	BioLegend
Anti-CD5	Rat IgG2 a,κ	(Ly-1)53-7-3	PE	5	Pharmigen
Streptavidin			PerCP-Cy5	5b	BD Bioscience
Anti-CD4	Rat IgG2 b,κ	GK1,5	PE	6	BioLegend
Anti-B220	Rat IgG2 a,κ	RA3-gB2	APC	6	BioLegend

Table S2. Murine antibodies used for the characterization of Spleen NK, T and B cell populations by flow cytometry.

A

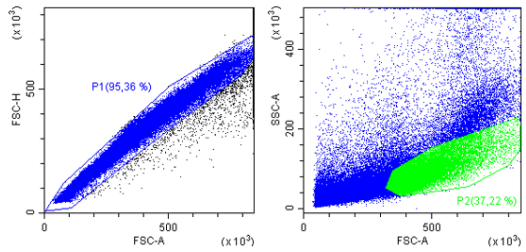
P1(95,36 %)
FSC-H
FSC-A
SSC-A
P2(37,22 %)

B

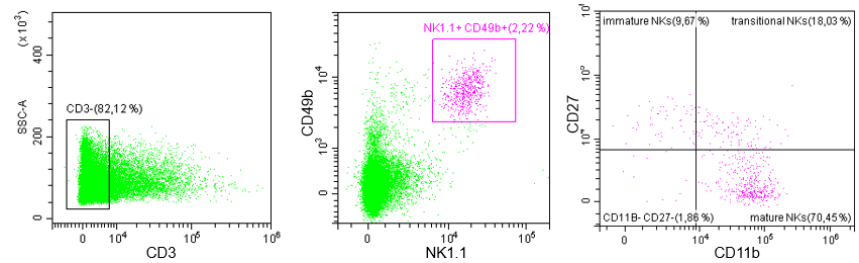
CD3-(82,12 %)
SSC-A
CD3
NK1.1+ CD49b+(2,22 %)
CD49b
NK1.1
immature NKs(9,67 %)
transitional NKs(18,03 %)
CD11B- CD27-(1,86 %)
mature NKs(70,45 %)
CD27
CD11b

C

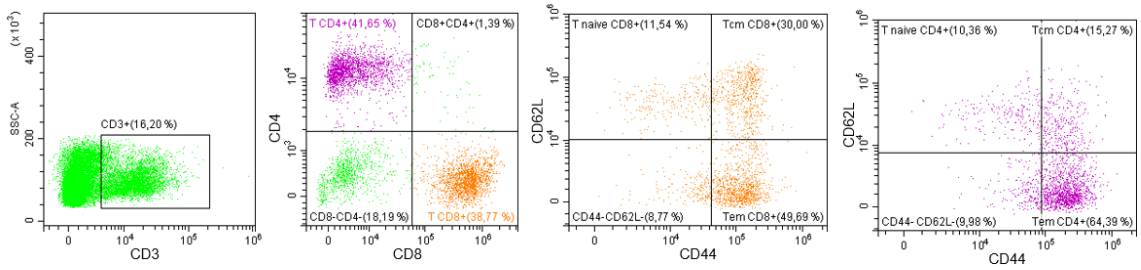
CD3+(16,20 %)
SSC-A
CD3
T CD4+(41,65 %)
CD8+CD4+(1,39 %)
CD8-CD4-(18,19 %)
T CD8+(38,77 %)
CD4
CD8
T naive CD8+(11,54 %)
Tcm CD8+(30,00 %)
CD44-CD62L-(8,77 %)
Tem CD8+(49,69 %)
CD62L
CD44
T naive CD4+(10,36 %)
Tcm CD4+(15,27 %)
CD44- CD62L-(9,98 %)
Tem CD4+(64,39 %)
CD62L
CD44

D

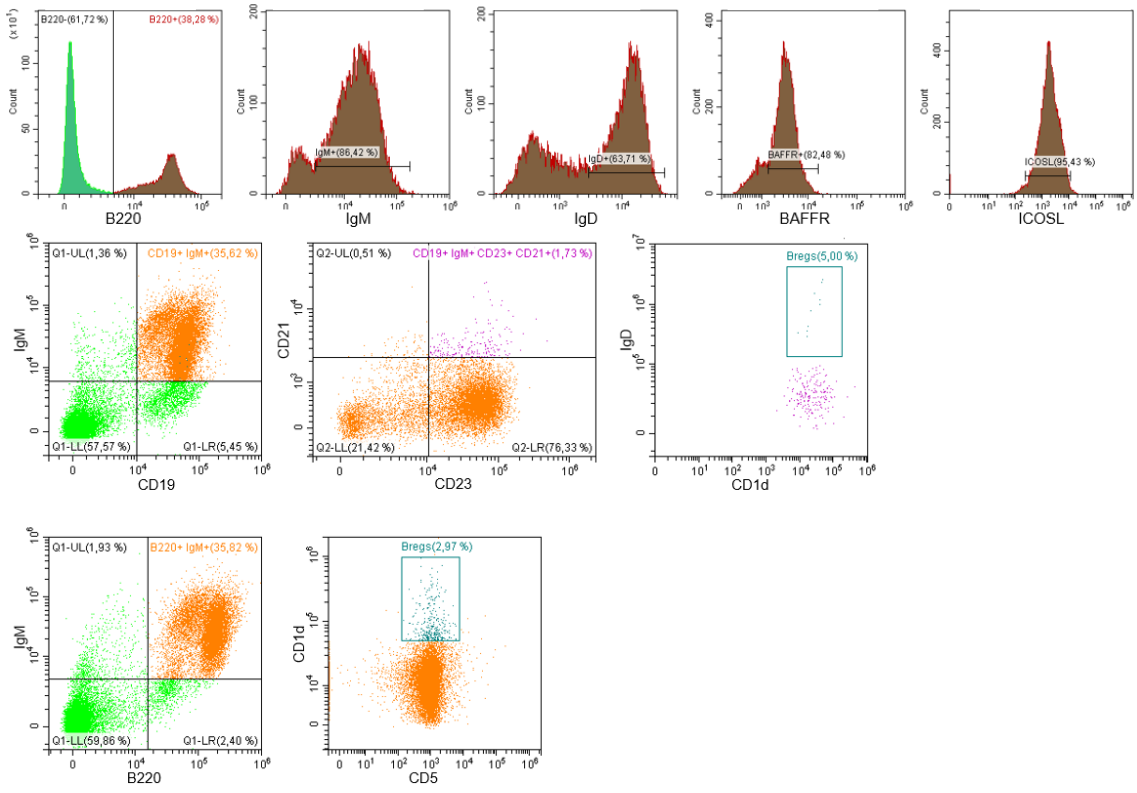
B220-(61,72 %)
B220+(38,28 %)
Count
B220
IgM+(86,42 %)
IgM
IgD+(63,71 %)
IgD
BAFFR+(82,48 %)
BAFFR
ICOSL(95,43 %)
ICOSL
Q1-UL(1,36 %)
CD19+ IgM+(35,82 %)
Q1-LL(57,57 %)
Q1-LR(5,45 %)
IgM
CD19
Q2-UL(0,51 %)
CD19+ IgM+ CD23+ CD21+(1,73 %)
Q2-LL(21,42 %)
Q2-LR(76,33 %)
CD21
CD23
Bregs(5,00 %)
IgD
CD1d
Q1-UL(1,93 %)
B220+ IgM+(35,82 %)
Q1-LL(59,86 %)
Q1-LR(2,40 %)
IgM
B220
Bregs(2,97 %)
CD1d
CD5

Figure S2. Gating strategy for the analysis of NK, T and B cell populations of the spleen.

Flow cytometry was performed on splenocytes from WT and BAMBI-KO mice. (**A**) P1 and P2 gating strategy (**B**) Gating strategy for the analysis of NK cells, including immature, transitional and mature subpopulations. (**C**) Gating strategy for the analysis of T cells, including memory subpopulations of CD8+ and CD4+ T cells. (**D**) Gating strategy for the analysis of B cells, including membrane molecules of B cells and Breg cells.